

## Pressure-induced $s \rightarrow d$ transfer and the equation of state of molybdenum

B. K. Godwal\* and Raymond Jeanloz

*Department of Geology and Geophysics, University of California, Berkeley, California 94720*

(Received 11 October 1989)

The equations of state of crystalline (bcc) and liquid molybdenum are calculated to pressure-temperature conditions of 600 GPa and 14 000 K with use of the linear muffin-tin orbitals (LMTO) model and corrected rigid-ion sphere (CRIS) model. Our results agree with those of previous work in documenting a pressure-induced shift of electrons from  $5s$  to  $4d$  states, especially above 100 GPa. An analysis of ultrasonic and shock-wave measurements, along with our theoretical findings, documents that the compressibility of bcc Mo becomes enhanced at pressures of 100–200 GPa. The enhanced compression, and possibly an anomalous increase in rigidity, are caused by the pressure-induced  $s \rightarrow d$  transfer. Our study reinforces the use of the Mo equation of state as a calibration standard for ultrahigh-pressure static experiments and, in particular, for the ruby-fluorescence technique.

### INTRODUCTION

The bonding character of molybdenum is expected to change at high pressures. Indeed, the recent discovery from Hugoniot sound-velocity measurements that Mo undergoes a structural transformation at about 210 GPa has been explained in terms of a transfer of conduction electrons from the  $5s$  to the  $4d$  band: the result is to stabilize the hcp relative to the bcc structure.<sup>1</sup> Our aim is to further examine this bonding change, concentrating on the equation of state at elevated pressure. We are motivated by the fact that the equation of state of bcc Mo plays a central role in the present calibration of the ruby-fluorescence technique used in ultrahigh-pressure static experiments.<sup>2</sup> Yet there is a well-established discrepancy between the equations of state derived from existing shock-wave data and high-precision ultrasonic measurements of the elastic moduli of bcc molybdenum.<sup>3</sup> Hence, we consider whether these data sets can be reconciled in terms of pressure-induced changes in elasticity reflecting changes in the electronic-band populations.

### THEORETICAL APPROACH

We calculate the equation of state of bcc molybdenum by theoretically evaluating the internal energy  $E$  as a function of volume  $V$  using the linear muffin-tin orbitals (LMTO) method of Andersen. The approach has been described previously,<sup>1,4,5</sup> and so it is only briefly summarized here. With neglect of electron-phonon interactions, the pressure is given by

$$P = -\partial E_c / \partial V + \gamma E_{lt} / V + \gamma_e E_e / V, \quad (1)$$

where  $E_c$  is the static-lattice (cold compression) energy,  $E_{lt}$  and  $E_e$  are the lattice vibrational (or thermal) and electronic contributions to the energy, and  $\gamma$  and  $\gamma_e$  are the vibrational and electronic Grüneisen parameters. The static-lattice energy is evaluated for the  $4d^5 5s^1$  configuration of valence electrons using the LMTO

method in the atomic-sphere approximation. The von Barth–Hedin exchange and correlation potential is employed,<sup>6</sup> and we retain angular-momentum components up to  $l=3$  in the calculation. Following Glötzel and McMahan,<sup>7</sup> the intercellular Coulomb interaction beyond the atomic-sphere approximation is accounted for through a muffin-tin correction to  $E_c$ . This correction increases with pressure, contributing between 1.5 and 3.0 GPa at  $V/V_0=1.0-0.5$  (subscript zero indicates zero pressure, throughout). In contrast, we do not correct for changes in core states during compression: the Kr configuration is kept frozen. We find from independent calculations<sup>8</sup> that the correction to the pressure due to the  $4s$  and  $4p$  core states is less than 1% of the total pressure throughout the range examined here, and so we ignore this effect.

The thermal contribution to the equation of state is derived from the last two terms in (1), with  $E_{lt}$  being approximated by the Debye-Grüneisen model as in Ref. 5. Specifically, we use the observed value<sup>9</sup> of Poisson's ratio, along with our calculated bulk modulus, to estimate the Debye temperature; this use of laboratory data reflects the fact that we obtain no information about shear moduli from our calculations. The vibrational Grüneisen parameter is obtained from the derivatives of our calculated equation of state by way of the Dugdale-MacDonald formula,<sup>10</sup> but our results would not be markedly changed were we to use the Slater<sup>11</sup> or free-volume<sup>12</sup> formulas for  $\gamma$ . Finally, the calculated density of states at the Fermi energy, and its volume derivative, yields the electronic pressure via  $E_e$  and  $\gamma_e$ , respectively.

Upon shock loading to high pressures and temperatures, molybdenum undergoes phase transformations:<sup>1</sup> first, to a new crystal structure thought to be hcp [referred to henceforth as hcp(?)] at 210 GPa, and then to the melt at Hugoniot pressures above 400 GPa. As there is no evidence of the crystal-structural transformation in the shock-wave (Hugoniot) equation of state,<sup>13</sup> we follow Hixson *et al.*<sup>1</sup> in assuming that the equations of state of the bcc and hcp(?) phases are identical. The liquid equa-

tion of state is obtained from the corrected rigid-ion sphere (CRIS) model,<sup>14</sup> which is based on effective interatomic potentials that are derived from our calculated isotherm for bcc Mo. The principal assumptions involved are that the interatomic potential in the dense fluid is taken to be the same as in the solid, for a given nearest-neighbor distance (corrected to the average coordination number in the melt), and this potential is taken to be central, pairwise additive, and extending only over nearest neighbors. Although the equations of state of the crystalline and liquid states of Mo are indistinguishable from the Hugoniot measurements,<sup>1,13</sup> we go through this exercise in order to obtain the internal energy of the melt, which differs greatly from that of the solid at the same volume (as illustrated by Fig. 5, below).

## RESULTS

The results of our calculations for the static lattice of bcc Mo are summarized in Figs. 1 and 2. We clearly see evidence for an increase upon compression in the  $d$ -like ( $n = 4$ ) electron population at the expense of the  $sp$ -like ( $n = 5$ ) electrons. This shift in the band populations begins at zero pressure, becoming significantly more rapid as pressure is increased above 100–200 GPa ( $V/V_0 < 0.8$ – $0.7$ ). Thus, our calculations are in complete accord with the experimental and theoretical results of Hixson *et al.*<sup>1</sup> in that the continuous increase of the  $d$ -electron population stabilizes the hcp structure at high pressures (we obtain an increase in the  $4d$  occupation of 0.45 electrons per atom between 0 and 320 GPa). The change in electronic structure must also soften the equation of state; that is, increase the compressibility relative

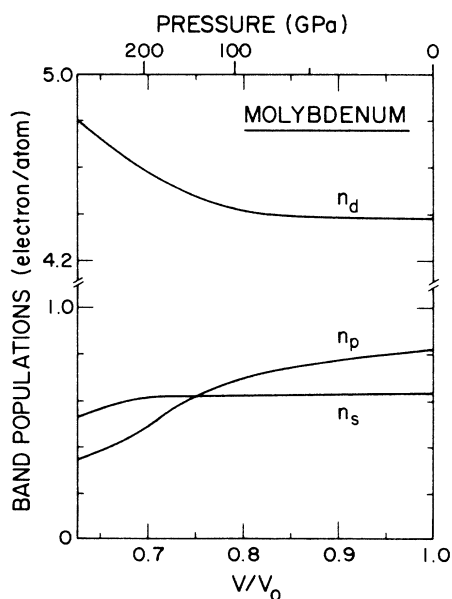


FIG. 1. Calculated electron populations in the  $4d$  ( $n_d$ ) and  $5sp$  ( $n_s, n_p$ ) bands of bcc Mo are shown as a function of volume. The  $5s$  and  $5p$  bands are treated as hybridized in the LMTO method. The calculated pressure of the static lattice is shown on the upper scale.

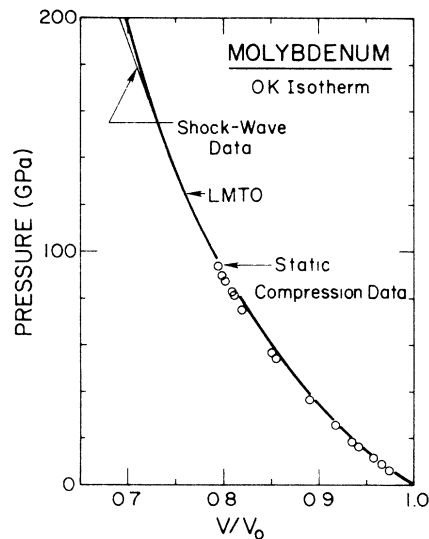


FIG. 2. Comparison of our calculated equation of state for bcc Mo (bold curve) with the results of shock-wave (Ref. 15) (thin curve) and static-compression (Ref. 2) (open circles) measurements, all reduced to the static lattice (0-K isotherm).

to what one would obtain for constant-band populations. This conclusion stems from the thermodynamic requirement that pressure stabilizes the state of reduced volume.

A comparison of the theoretical equation of state with that observed by shock-wave<sup>15</sup> and static<sup>2</sup> compression, thermally corrected to the 0-K isotherm, shows that our results are in good agreement with existing high-pressure measurements on the bcc structure (Fig. 2). The static-compression data are not entirely independent from the shock-wave measurements because the latter were used as part of the pressure calibration for the former. Nevertheless, as the ruby-fluorescence calibration of static pressures is based on shock-wave equations of state for four different metals,<sup>2</sup> our comparison with the static measurements on Mo remains meaningful. Also, the possible influence of nonhydrostaticity in the static experiments is expected to be small.<sup>2,3</sup> Thus, the final deviation of the calculated equation of state from either the shock-wave or the static-compression data is found to be well within the experimental uncertainties over the compressions studied.

A more detailed comparison between theory and experiment is possible at ambient conditions of zero pressure and 300 K (Table I). We find that although the agreement in volume  $V_0$ , isothermal bulk modulus  $B_{0T}$ , and its pressure derivative  $B'_{0T}$  is within 1.5, 5.5, and 11 %, respectively, the deviations are about 4–10 times greater than the experimental uncertainties. Still, this is sufficiently good agreement for our purposes. Similarly, the calculated thermal properties described by the Debye temperature  $\Theta_0$  and lattice Grüneisen parameter  $\gamma_0$  are in relatively good accord with the data.

It is only in the case of the electronic Grüneisen parameter  $\gamma_{e0}$  that we deviate significantly from the experimental value, which is obtained from low-temperature thermal expansion measurements.<sup>16</sup> We predict a value

TABLE I. Properties of molybdenum at 300 K,  $P=0$ .

	Theory <sup>a</sup>	Experiment
Volume, $V_0$ (cm <sup>3</sup> /mol)	9.536	9.391 ( $\pm 0.009$ ) <sup>b</sup>
$s$ (a.u.) <sup>c</sup>	2.9438	2.929 ( $\pm 0.001$ )
Bulk modulus, $B_{0T}$ (GPa)	275.3	260.8 ( $\pm 0.8$ ) <sup>b</sup>
$B'_{0T}$	4.0	4.46 ( $\pm 0.13$ ) <sup>b</sup>
Debye temperature, $\Theta_0$ (K)	480	450 ( $\pm 5$ ) <sup>d</sup>
Grüneisen parameter		
Lattice, $\gamma_0$	1.78	1.55 ( $\pm 0.05$ ) <sup>b</sup>
Electronic, $\gamma_{0e}$	0.45	1.5 ( $\pm 0.3$ ) <sup>e</sup>

<sup>a</sup>This study: LMTO calculations with lattice vibrational correction.

<sup>b</sup>Reference 9.

<sup>c</sup> $4\pi s^3/3 = V_0$ .

<sup>d</sup>Reference 29.

<sup>e</sup>Reference 16.

smaller than the free electron  $\gamma_e = \frac{2}{3}$ , and this is, in turn, much less than the observed value. It may be that our calculated values of the electronic Grüneisen parameter are reasonable for compressed Mo: a small value would not be surprising for a  $d$ -electron metal, but this explanation implies that the observed  $\gamma_e$  is anomalously large at zero pressure. Alternatively, the discrepancy between the calculated and observed  $\gamma_{e0}$  may simply reflect the true reliability of the LMTO method, as applied here (e.g., in the neglect of electron-photon interactions<sup>17</sup>). In any case, the electronic contribution to the pressure is sufficiently small at the temperatures considered in this study that a threefold error in the electronic Grüneisen parameter does not affect our conclusions.

In order to compare theory with the highest-pressure data available, we calculate the shock-wave equation of state by combining the Hugoniot equations<sup>15</sup> with our Debye-Grüneisen model for crystalline Mo. The individual contributions to the calculated Hugoniot pressure, the electronic, lattice thermal, and (by difference) cold compression terms in (1), are shown in Fig. 3. Our con-

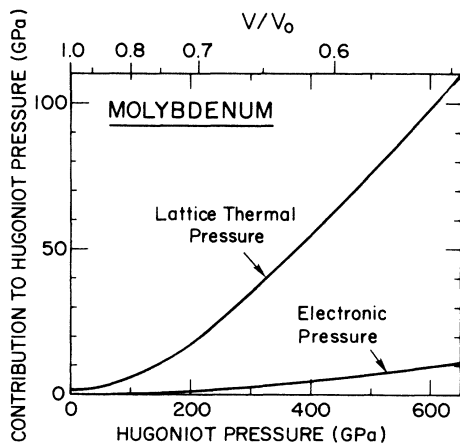


FIG. 3. Calculated contributions to the Hugoniot pressure of crystalline Mo: the lattice-thermal (or lattice-vibrational) contribution and the electronic contribution are shown as functions of the total Hugoniot pressure (lower scale) and the volume (upper scale).

clusion that the electronic pressure is negligible, even if poorly determined by the theory, is substantiated here; we estimate that it amounts to no more than 1% of the total pressure in the solid state. In contrast, the lattice thermal contribution to the pressure is on the order of 10% at shock pressures above 200 GPa. We have similarly combined the Hugoniot equations with our liquid-state model to derive the shock-compression curve for the melt, and the combined results for solid and liquid Mo are summarized in Fig. 4.

Expressing the Hugoniot equation of state in terms of the primary variables of shock experiments, the shock-wave velocity  $U_s$  and the particle velocity  $u_p$ , it is clear from Fig. 4 that the theory matches well with the available data for molybdenum. As expected, we find that the Hugoniot of the liquid and solid phases are nearly indistinguishable at high pressures. In addition, these describe a linear  $U_s$ - $u_p$  trend, as is commonly found for shock-wave measurements on elements.<sup>15,18</sup> What is less evident, however, is that the intercept and slope of the  $U_s$ - $u_p$  equation of state are systematically larger and smaller, respectively, than would be expected from the ultrasonic measurements<sup>9</sup> of the compressional moduli.<sup>18,19</sup> This discrepancy applies to both the theoretical and experimental results in Fig. 4. We return to the disagreement between the results of infinitesimal-compression (ultrasonic) and finite-compression (shock-wave and static-compression) measurements of the compressional moduli in the next section.

As a final application of our theoretical model for crystalline and liquid Mo, we calculate the Hugoniot temperatures for both phases.<sup>15</sup> Also, following Ref. 1, we estimate the melting temperature of molybdenum by way of the Lindemann relation. The results, plotted in Fig. 5, show that the pressure at which melting is observed under shock compression is in rough agreement with what we calculate. Specifically, given the approximations in

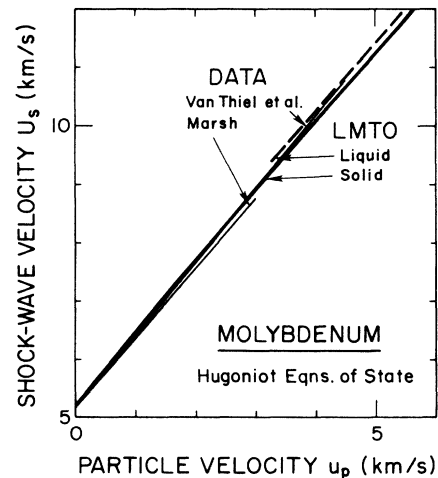


FIG. 4. Comparison of calculated shock-wave (Hugoniot) equation of state of molybdenum (bold solid and dashed curves refer to solid and liquid phases, respectively) with two fits to existing data (thin curves) (Refs. 13 and 21).

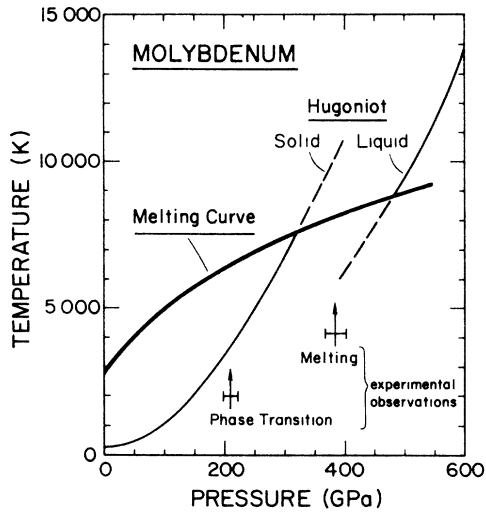


FIG. 5. Calculated melting temperature (bold curve), and Hugoniot temperatures for solid and liquid Mo (thin curves) shown as functions of pressure. The experimentally observed pressures (Ref. 1) at which Mo undergoes a solid-solid phase transition and melting along the Hugoniot are shown by arrows (along with uncertainties) near the bottom.

our analysis (e.g., no energy of transformation at 210 GPa, neglect of anharmonicity beyond the quasiharmonic approximation, and use of the Lindemann expression), as well as the possible uncertainties in the data (e.g., metastable superheating during shock melting), the  $\sim 50$ -GPa agreement between theory and experiment is acceptable. As more data become available for Mo at ultrahigh pressures and temperatures, notably measurements of Hugoniot and melting temperatures as functions of pressure, Fig. 5 will offer an especially stringent test of our calculations.

### DISCUSSION

The adiabatic compression curves derived from ultrasonic and shock-wave measurements on molybdenum clearly illustrate the discrepancy between the results obtained from these two different types of experiments (Fig. 6). By 50–60 GPa, the best-fit isentrope to the Hugoniot begins to deviate to smaller volumes that are well outside the uncertainties of the ultrasonically based adiabat. This is shown with greater clarity in Fig. 7, which gives Birch's<sup>20</sup> normalized pressure

$$F = P / [3f(1+2f)^{2.5}]$$

as a function of the Eulerian finite-strain variable

$$f = [(V/V_0)^{-2/3} - 1] / 2.$$

In the Eulerian finite-strain formulation, the normalized pressure is a polynomial in the strain

$$F = B_0[1 + a_1f + a_2f^2 + \dots], \quad (2)$$

with

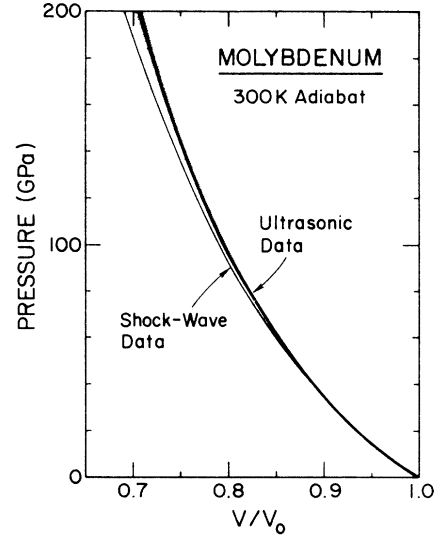


FIG. 6. Experimentally based adiabatic equation of state for bcc Mo, showing pressure as a function of volume upon isentropic compression from ambient conditions. The adiabat obtained from a reduction of Hugoniot data (Ref. 15) (thin curve) is compared with that obtained from the ultrasonically measured adiabatic moduli (Ref. 9) (bold curve; shading indicates the estimated uncertainty). The latter is derived from the ultrasonic moduli by way of the third-order Eulerian finite-strain expression [i.e.,  $a_2 = 0$  in (2)].

$$a_1 = 3(B'_0 - 4) / 2, \quad (3)$$

$$a_2 = 3[B_0B''_0 + B'_0(B'_0 - 7) + \frac{143}{9}] / 2 \quad (4)$$

being the third-order and fourth-order terms, respectively.<sup>18,20</sup> For comparison, we have used the third-order form of (2) to derive the equation of state of bcc Mo from the ultrasonically determined moduli. Thus, the observed adiabatic compression, as deduced from the shock-wave data, defines a much softer equation of state than would be expected from the ultrasonic measurements. Above about 130 GPa, the ultrasonic and shock-derived adiabats differ by more than their combined uncertainties (Fig. 7). The result is that the adiabatic values  $B_{0S}$  and  $B'_{0S}$  inferred from the Hugoniot data,<sup>15,21</sup> corresponding to the slope and intercept at  $f = 0$  in Fig. 7, are, respectively, larger and smaller than the exact values obtained ultrasonically.

Because the ultrasonic measurements<sup>9</sup> were carried out only to 0.5 GPa, they cannot reflect the changes in electronic-band populations that occur primarily above 100 GPa (Fig. 1). Thus, the simplest reconciliation of the ultrasonic results with the shock-wave (and static-compression) data is to invoke a softening of the equation of state of bcc Mo due to the  $5s \rightarrow 4d$  electron transfer at finite compressions. This softening can be accommodated in the Eulerian finite-strain equation of state by adding the fourth-order term (4) in the expansion (2). Simultaneously fitting the Hugoniot data<sup>21</sup> and the ultrasonic measurements (with parameters  $B_{0S} = 262.5 \pm 0.6$  GPa and  $a_1 = 0.7 \pm 0.2$ ), we obtain the adiabatic value of

$a_2 = -6.8 \pm 1.2$  and thus  $B_{0S} B''_{0S} = -9.1 \pm 0.8$  from a weighted least-squares analysis.

As shown in Fig. 7, the fourth-order equation of state derived from these parameters satisfies all of the available data. We note that our value for the fourth-order term implies a shift in  $B'$  of only 0.02 between pressures of 0 and 0.5 GPa. This shift is much smaller than the uncertainty of 0.1 estimated for the ultrasonic measurement of  $B'$ , so the  $a_2$  contribution would not have been noticeable in the experiment of Ref. 9. Furthermore, our refinement of the equation of state for bcc molybdenum does not affect the calibration of the ruby-fluorescence scale because the pressure shift of the ruby fluorescence is constrained directly by the reduced Hugoniot data.<sup>2</sup> Instead, the incorporation of a fourth-order term, reflecting the softening of the equation of state at elevated pressures, brings the ruby-fluorescence calibration and the ultrasonic measurements on Mo into mutual agreement.

We recognize that the softening, or enhanced compression, of the equation of state associated with the bonding change affects the vibrational Grüneisen parameter because of the dependence of  $\gamma$  on the first and second derivatives of the  $P$ - $V$  curve.<sup>22</sup> In the present case the

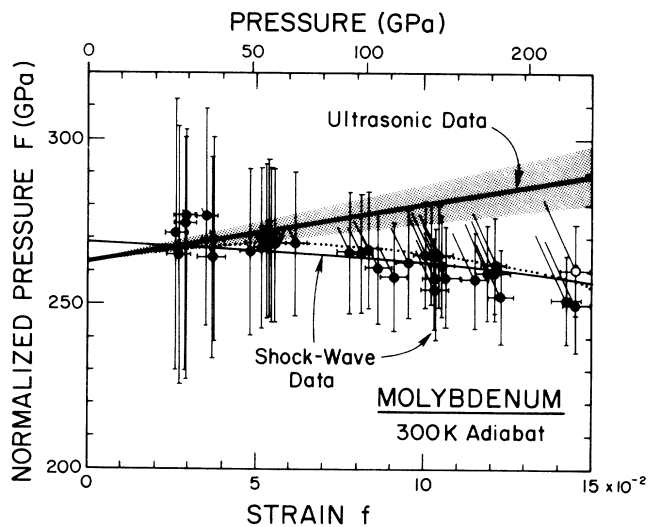


FIG. 7. Experimentally based adiabatic equation of state for bcc Mo, showing Birch's (Ref. 20) normalized pressure  $F$  as a function of the Eulerian finite-strain measure  $f$  upon isentropic compression from ambient conditions (the corresponding pressure is given on the upper scale). The shock-wave adiabat (thin curve) and ultrasonic adiabat (bold curve; shading indicates the estimated uncertainty) are identical to those in Fig. 6. The Hugoniot data of Ref. 21 are shown reduced to the adiabat according to the Mie-Grüneisen approach described in Refs. 30 and 31 (circles with error bars), with the end of the diagonal tie line on each point showing the  $F$ - $f$  value for the raw Hugoniot measurement. The open point at  $f = 0.145$  represents a datum that may be at sufficiently high pressures to be in the high-pressure (hcp?) crystalline phase (Ref. 1). The dotted curve is the fourth-order Eulerian finite-strain adiabat that is fitted to the (reduced) Hugoniot measurements (Ref. 21) and the low-pressure ultrasonic data (Ref. 9).

effect is subtle, amounting to a decrease in the logarithmic volume derivative of  $\gamma$  from a high value ( $q \sim 1.9$ ) at low compressions ( $1.0 > V/V_0 > 0.8$ ) to a more typical value of  $q \sim 0.9$  at high compressions ( $V/V_0 < 0.8$ ). This change in  $q$  is accounted for in our calculation of the high-pressure vibrational Grüneisen parameter, but it does not have any quantitatively noticeable influence on our calculations or analyses of Hugoniot data. Still, it is noteworthy that the large initial value of  $q$  is in good agreement with a recent investigation of the high-temperature bulk modulus of molybdenum at zero pressure.<sup>23</sup>

The Hugoniot sound-velocity measurements of Hixson *et al.*<sup>1</sup> offer independent support for the proposal that the elastic moduli of bcc Mo are affected by the  $s \rightarrow d$  transfer of electrons at high compressions. Displaying their data as Poisson's ratio  $\nu$  versus pressure, three anomalies are evident (Fig. 8). First, the observed values of  $\nu$  decrease with increasing pressure below 210 GPa; then, there is an abrupt change in slope at about 210 GPa; and finally, Poisson's ratio is seen to increase suddenly to  $\nu \sim 0.5$  near 400 GPa. The second and third of these anomalies are well explained by solid-solid and solid-liquid transitions, as discussed by Hixson *et al.*<sup>1</sup>

The decrease in Poisson's ratio observed between 150 and 200 GPa is not so easily explained, however, because the effect of pressure is normally to increase rather than decrease  $\nu$ . That is, the shear modulus should increase less rapidly than the bulk modulus on compression, contrary to what is shown for bcc Mo above 150 GPa (Fig. 8). For example, if the effects of phase transitions and strength are discounted, Poisson's ratio has been ob-

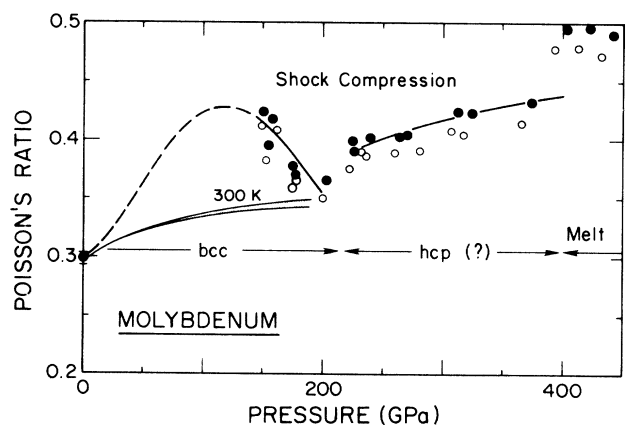


FIG. 8. Poisson's ratio of molybdenum as a function of pressure. Circles show the results of Hugoniot sound-velocity measurements (Ref. 1), both as analyzed in Ref. 1 (solid symbols) and as derived using the Hugoniot fits given in Ref. 21 (open symbols): the agreement between the two analyses illustrates the reliability of the values shown (thin curve, dashed where interpolated). The shaded curve gives the expected change in Poisson's ratio with isothermal compression of the bcc phase of Mo, as obtained from the ultrasonically measured elastic moduli (Ref. 9) and third-order Eulerian finite-strain theory (Ref. 20). The inferred ranges of Hugoniot pressures for two crystalline phases (bcc and hcp?) and melt are also indicated (Ref. 1).

served to increase in previous measurements of Hugoniot sound velocities (e.g., Refs. 24 and 25). Moreover, our expectation that  $v$  increases with pressure is illustrated by the ultrasonic measurements, as shown in Fig. 8. Note that it is the average value of Poisson's ratio, corresponding to the isotropic aggregate value of the shear modulus, that is pertinent here; thus,  $\nu$  depends on a combination of all of the single-crystal moduli.<sup>26</sup> The additional effect of temperature increasing along the Hugoniot (Fig. 5) can only serve to increase Poisson's ratio further.

One possible explanation is that the bcc phase transforms continuously to the hcp(?) phase between 150 and 200 GPa. The decrease in  $\nu$  would then simply reflect an increase with pressure in the amount of the new phase that is present relative to the bcc structure. We consider this hypothesis implausible, however, because pressure-induced bcc $\leftrightarrow$ hcp transitions are known to occur with little hindrance in elements.<sup>27</sup> This conclusion holds especially for shock compression, in which local shearing can induce the transformation, as is nicely illustrated by the  $\alpha \rightarrow \epsilon$  transition in Fe.<sup>28</sup>

Two additional effects that we ignore are the influence of textures (preferred crystallographic orientation) and the possible existence of a second high-pressure phase, other than the hcp(?) or the original bcc phases, between 150 and 200 GPa. Primarily, we ignore these possibilities because there is no independent evidence for either (e.g., from the observed Hugoniot equation of state).<sup>21</sup> In addition, it is unlikely that the average Poisson's ratio that is derived from the Hugoniot sound-velocity measurements

can be sufficiently influenced by texturing of bcc Mo to yield the observed magnitude of the decrease in  $\nu$  at high pressures.<sup>26</sup> Similarly, the enhanced compressibility of molybdenum at high pressures is too subtle to influence the vibrational Grüneisen parameter enough to affect the results shown in Fig. 8 (see also, Ref. 1).

The shock-wave data suggest, therefore, that Poisson's ratio of bcc Mo decreases anomalously at approximately the same pressures that the  $s \rightarrow d$  transfer becomes significant. The increase in  $d$  character with compression apparently contributes to increasing the shear modulus and, relatively speaking, to softening the equation of state. As noted by Katahara *et al.*,<sup>9</sup> a large increase in shear modulus with pressure is typically associated with a small value of the electronic Grüneisen parameter; this is consistent with our calculated results. Moreover, a softening of the equation of state caused by a bonding change reconciles the existing elasticity and high-pressure equation of state data for molybdenum.

#### ACKNOWLEDGEMENTS

We thank M. H. Manghnani, J. A. Moriarty, and J. W. Shaner for helpful discussions, as well as R. S. Hixson for supplying the experimental results prior to publication. This work was supported by the Institute of Geophysics and Planetary Physics (IGPP) of Lawrence Livermore National Laboratory (LLNL) and by the National Science Foundation.

\*Permanent address: Neutron Physics Division, Bhabha Atomic Research Center, Trombay, Bombay 400085, Maharashtra, India.

<sup>1</sup>R. S. Hixson, D. A. Boness, J. W. Shaner, and J. A. Moriarty, *Phys. Rev. Lett.* **62**, 637 (1989).

<sup>2</sup>H. K. Mao, P. M. Bell, J. W. Shaner, and D. J. Steinberg, *J. Appl. Phys.* **49**, 3276 (1978).

<sup>3</sup>K. W. Katahara, M. H. Manghnani, L. C. Ming, and E. S. Fisher, in *High-Pressure Research*, edited by M. H. Manghnani and S. Akimoto (Academic, New York, 1977), p. 351.

<sup>4</sup>H. L. Skriver, *The LMTO Method* (Springer, Berlin, 1984).

<sup>5</sup>B. K. Godwal and R. Jeanloz, *Phys. Rev. B* **40**, 7501 (1989).

<sup>6</sup>U. von Barth and L. Hedin, *J. Phys. C* **5**, 1629 (1972).

<sup>7</sup>D. Glötzel and A. K. McMahan, *Phys. Rev. B* **20**, 3210 (1979).

<sup>8</sup>S. K. Sikka and B. K. Godwal, *Phys. Rev. B* **35**, 1446 (1987).

<sup>9</sup>K. W. Katahara, M. H. Manghnani, and E. S. Fisher, *J. Phys. F* **9**, 773 (1979).

<sup>10</sup>J. S. Dugdale and D. K. MacDonald, *Phys. Rev.* **85**, 832 (1953).

<sup>11</sup>J. C. Slater, *Introduction to Chemical Physics* (McGraw-Hill, New York, 1939) [also (Dover, New York, 1970)].

<sup>12</sup>V. Vaschenko and V. N. Zubarev, *Fiz. Tverd. Tela* (Leningrad) **5**, 886 (1963) [*Sov. Phys.—Solid State* **5**, 643 (1963)].

<sup>13</sup>*Compendium of Shock Wave Data*, edited by M. van Thiel, J. Shaner, and E. Salinas [UCRL-50108, Lawrence Livermore National Laboratory, 1977 (unpublished)].

<sup>14</sup>G. I. Kerley, *J. Chem. Phys.* **73**, 469 (1980); **73**, 478 (1980).

<sup>15</sup>R. G. McQueen, S. P. Marsh, J. W. Taylor, J. N. Fritz, and J.

W. Carter, in *High Velocity Impact Phenomena*, edited by R. Kinslow (Academic, New York, 1970), p. 293.

<sup>16</sup>R. S. Krishnan, R. Srinivasan, and S. Devanarayanan, *Thermal Expansion of Crystals* (Pergamon, New York, 1979).

<sup>17</sup>D. C. Wallace, *Thermodynamics of Crystals* (Wiley, New York, 1972).

<sup>18</sup>R. Jeanloz, *J. Geophys. Res.* **94**, 5873 (1989).

<sup>19</sup>D. J. Steinberg, *J. Phys. Chem. Solids* **43**, 1173 (1982).

<sup>20</sup>F. Birch, *J. Geophys. Res.* **83**, 1257 (1978).

<sup>21</sup>*LASL Shock Hugoniot Data*, edited by S. P. Marsh (University of California Press, Berkeley, 1980).

<sup>22</sup>M. Ross and A. K. McMahan, *Phys. Rev. B* **26**, 4088 (1982).

<sup>23</sup>G. H. Miller, T. J. Ahrens, and E. M. Stolper, *J. Appl. Phys.* **63**, 4469 (1988).

<sup>24</sup>J. M. Brown and R. G. McQueen, *J. Geophys. Res.* **91**, 7485 (1986).

<sup>25</sup>J. W. Shaner, J. M. Brown, C. A. Swenson, and R. G. McQueen, *J. Phys. (Paris) Colloq.* **45**, C8-235 (1984).

<sup>26</sup>M. J. P. Musgrave, *Crystal Acoustics* (Holden-Day, San Francisco, 1970).

<sup>27</sup>R. M. Wentzcovitch and M. L. Cohen, *Phys. Rev. B* **37**, 5571 (1988).

<sup>28</sup>W. A. Bassett and E. Huang, *Science* **238**, 780 (1987).

<sup>29</sup>*American Institute of Physics Handbook*, 3rd ed., edited by D. E. Gray (McGraw-Hill, New York, 1972).

<sup>30</sup>D. L. Heinz and R. Jeanloz, *J. Appl. Phys.* **55**, 885 (1984).

<sup>31</sup>T. J. Ahrens and R. Jeanloz, *J. Geophys. Res.* **92**, 10363 (1987).

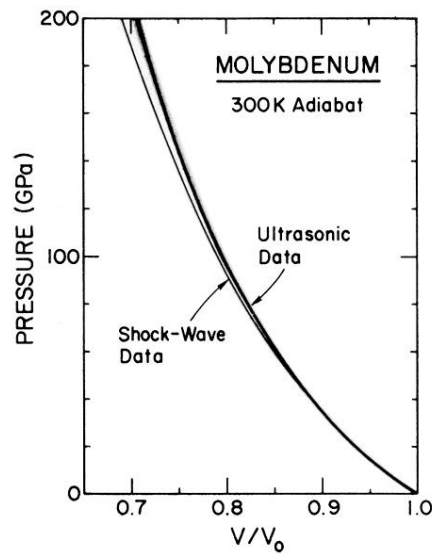


FIG. 6. Experimentally based adiabatic equation of state for bcc Mo, showing pressure as a function of volume upon isentropic compression from ambient conditions. The adiabat obtained from a reduction of Hugoniot data (Ref. 15) (thin curve) is compared with that obtained from the ultrasonically measured adiabatic moduli (Ref. 9) (bold curve; shading indicates the estimated uncertainty). The latter is derived from the ultrasonic moduli by way of the third-order Eulerian finite-strain expression [i.e.,  $a_2=0$  in (2)].

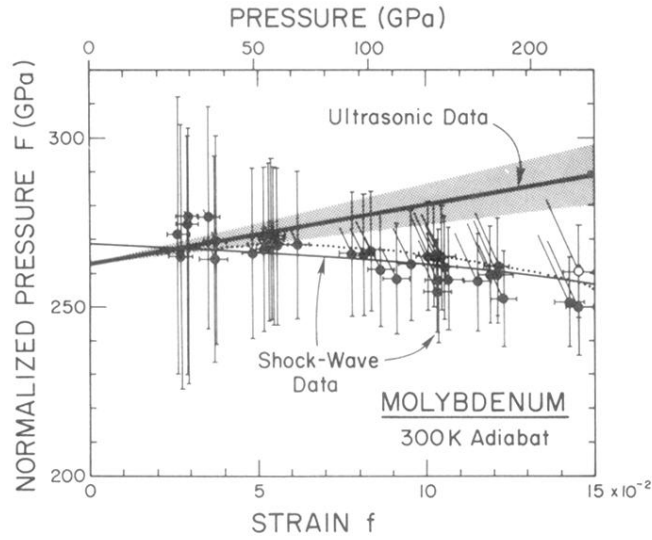


FIG. 7. Experimentally based adiabatic equation of state for bcc Mo, showing Birch's (Ref. 20) normalized pressure  $F$  as a function of the Eulerian finite-strain measure  $f$  upon isentropic compression from ambient conditions (the corresponding pressure is given on the upper scale). The shock-wave adiabat (thin curve) and ultrasonic adiabat (bold curve; shading indicates the estimated uncertainty) are identical to those in Fig. 6. The Hugoniot data of Ref. 21 are shown reduced to the adiabat according to the Mie-Grüneisen approach described in Refs. 30 and 31 (circles with error bars), with the end of the diagonal tie line on each point showing the  $F$ - $f$  value for the raw Hugoniot measurement. The open point at  $f = 0.145$  represents a datum that may be at sufficiently high pressures to be in the high-pressure (hcp?) crystalline phase (Ref. 1). The dotted curve is the fourth-order Eulerian finite-strain adiabat that is fitted to the (reduced) Hugoniot measurements (Ref. 21) and the low-pressure ultrasonic data (Ref. 9).



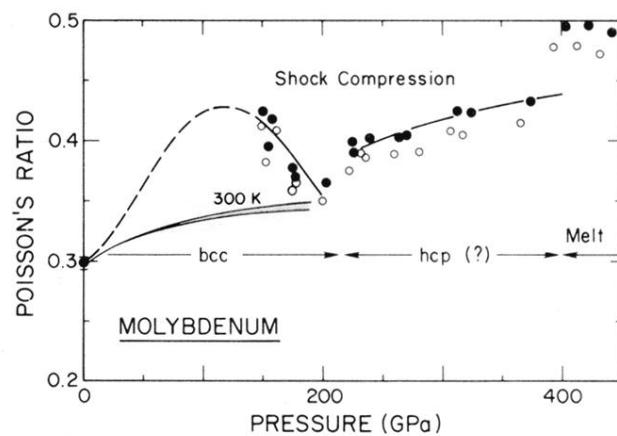


FIG. 8. Poisson's ratio of molybdenum as a function of pressure. Circles show the results of Hugoniot sound-velocity measurements (Ref. 1), both as analyzed in Ref. 1 (solid symbols) and as derived using the Hugoniot fits given in Ref. 21 (open symbols): the agreement between the two analyses illustrates the reliability of the values shown (thin curve, dashed where interpolated). The shaded curve gives the expected change in Poisson's ratio with isothermal compression of the bcc phase of Mo, as obtained from the ultrasonically measured elastic moduli (Ref. 9) and third-order Eulerian finite-strain theory (Ref. 20). The inferred ranges of Hugoniot pressures for two crystalline phases (bcc and hcp?) and melt are also indicated (Ref. 1).